

# A Wireless Neural Interface for Chronic Recording

Reid R. Harrison<sup>1,2</sup>, Ryan J. Kier<sup>1</sup>, Sohee Kim<sup>1</sup>  
Loren Rieth<sup>1</sup>, David J. Warren<sup>2</sup>, Noah M. Ledbetter<sup>2</sup>  
Gregory A. Clark<sup>2</sup>, Florian Solzbacher<sup>1,2</sup>

<sup>1</sup>Department of Electrical & Computer Engineering

<sup>2</sup>Department of Bioengineering

University of Utah  
Salt Lake City, UT USA

Cynthia A. Chestek<sup>3</sup>, Vikash Gilja<sup>4</sup>, Paul Nuyujukian<sup>5</sup>  
Stephen I. Ryu<sup>6</sup>, Krishna V. Shenoy<sup>3,7</sup>

<sup>3</sup>Department of Electrical Engineering

<sup>4</sup>Department of Computer Science, <sup>5</sup>School of Medicine

<sup>6</sup>Department of Neurosurgery, <sup>7</sup>Neurosciences Program  
Stanford University  
Stanford, CA USA

**Abstract**—A primary goal of the Integrated Neural Interface Project (INIP) is to develop a wireless, implantable device capable of recording neural activity from 100 micromachined electrodes. The heart of this recording system is a low-power integrated circuit that amplifies 100 weak neural signals, detects spikes with programmable threshold-crossing circuits, and returns these data via digital radio telemetry. The chip receives power, clock, and command signals through a coil-to-coil inductive link. Here we report that the isolated integrated circuit successfully recorded and wirelessly transmitted digitized electrical activity from peripheral nerve and cortex at 15.7 kS/s. The chip also simultaneously performed accurate on-chip spike detection and wirelessly transmitted the spike threshold-crossing data. We also present preliminary successful results from full system integration and packaging.

## I. INTRODUCTION

A primary goal of the Integrated Neural Interface Project (INIP) at the University of Utah is the development of a wireless, implantable neural recording device for medical and scientific applications. The Integrated Neural Interface (INI) under development can utilize either a Utah Electrode Array (UEA) or Utah Slanted Electrode Array (USEA) to make contact with neural tissue. These MEMS devices typically consist of  $10 \times 10$  arrays with an electrode-to-electrode spacing of 400  $\mu\text{m}$  and electrode lengths between 0.5 and 1.5 mm [1].

Over the past four years, we have been developing a stand-alone integrated circuit (IC) that will be flip-chip bonded to the back of a UEA or USEA to amplify, digitize, and transmit neural signals out of the body wirelessly [2,3]. Power, clock, and command signals are sent to the chip wireless via an inductive coil-to-coil link. Power dissipation of the chip is severely limited in order to prevent tissue damage due to chronic heating.

In this paper, we present the latest results from INIP, including a fully-functioning neural-recording IC that has obtained signals from both peripheral nerve and cerebral cortex in wireless recording experiments. We also present preliminary successful test results of a fully integrated system with IC, electrode array, power coil, and coatings. These

integration tests used an earlier version of the IC that was not fully functional, but was able to transmit an RF carrier frequency to validate chip operation under wireless power.

## II. INTEGRATED CIRCUIT RESULTS

### A. Chip Design

The latest version of our 100-channel wireless neural recording IC is designated INI5, and was fabricated in a commercially available 0.6- $\mu\text{m}$  2P3M BiCMOS process. Six 15-cm wafers were fabricated, and some die were packaged in plastic quad flat pack (QFP) packages for non-implanted experiments (Fig. 1). The bare die measures  $4.6 \times 5.4 \text{ mm}^2$ , with much of this area consumed by an array of 100 neural signal amplifiers (0.25–5 kHz bandwidth) and spike detectors.

Design details of this family of integrated circuits have been published previously [2,3]. In past chips, design errors resulted in only partial functionality of the chip. With INI5, all design errors have been corrected, so a wider range of chip operation can be demonstrated. The input-referred noise of each amplifier during wireless powering (measured with the amplifier input tied to ground) is 5  $\mu\text{V}_{\text{rms}}$ . The chip consumes 8 mW from an unregulated AC coil voltage that is rectified and regulated on chip to 3.0 VDC.

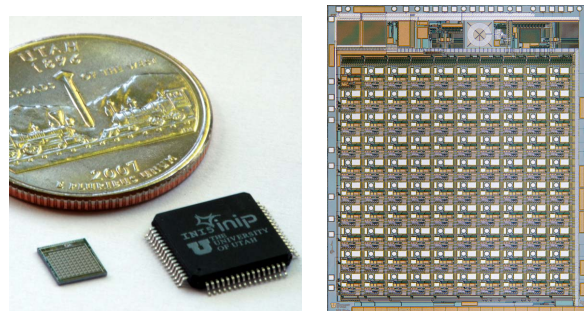


Figure 1. **Left:** INI5 integrated circuit in bare die form and packaged in a plastic QFP package, with a US quarter for scale. **Right:** Microphotograph of INI5 chip, measuring  $4.6 \times 5.4 \text{ mm}^2$ . A  $10 \times 10$  array of neural signal amplifiers and spike detectors occupies the center of the chip; the top circuitry includes a voltage rectifier and regulator, clock and data recovery circuits, a 10-bit ADC, and a 900-MHz digital FSK transmitter.

This work was supported by NIH/NINDS contract N01-NS-4-2362, and by the Johns Hopkins Applied Physics Laboratory under the DARPA Revolutionizing Prosthetics program contract N66001-06-C-8005.

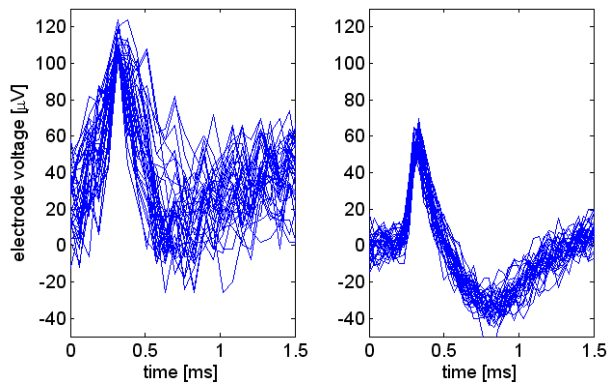


Figure 2. Time-aligned action potentials recorded in cat sciatic nerve by IN15 chip (left) and conventional Cerebus system (right), recorded within 1 h of each other.

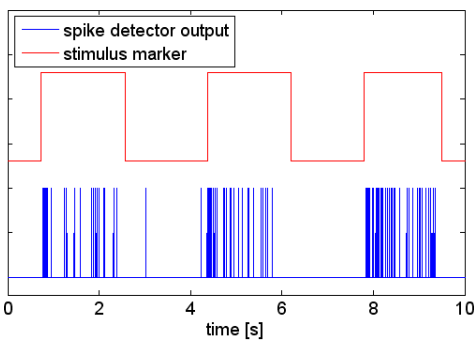


Figure 3. Output from on-chip spike detector (from wireless telemetry) during manual Achilles tendon stretch, with the spike detection threshold set to  $+99 \mu\text{V}$ . The spikes detected by the IN15 chip correlate well with the stimulus marker.

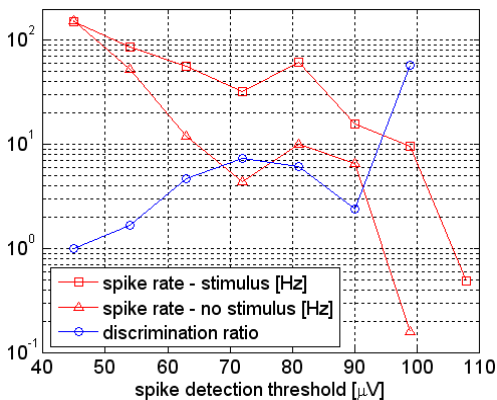


Figure 4. Rates of spike detection from IN15 with Achilles tendon stretch stimulus present and absent, for various spike detection thresholds. The discrimination ratio is the ratio of spike rates.

### B. Peripheral Nerve Recording

In brief, using wireless power, commands, and telemetry, IN15 successfully recorded and wirelessly transmitted digitized electrical activity from cat sciatic nerve at  $15.7 \text{ kS/s}$ . IN15 also simultaneously performed accurate on-chip spike detection and wirelessly transmitted the spike threshold-crossing data. Both raw spike firing rates and the number of

on-chip spike detections were highly correlated with manual stimulation of the cat's foot.

To validate proper operation of the IN15 chip, we used a QFP-packaged, non-implanted version of the chip to record action potentials from a USEA implanted in the sciatic nerve in the left leg of an anesthetized cat. The IN15 chip was attached to the array via two wires: one connected to an intraneural electrode, and the other connected to a nearby implanted electrical reference. Other than the USEA, the only off-chip components connected to the IN15 chip were a 5.8-cm power receive coil and a 10-nF capacitor used to smooth the rectified coil voltage before on-chip voltage regulation. Power was delivered using a second 5.8-cm coil driven with a  $2.765 \text{ MHz}$ ,  $\sim 60 \text{ V}_{\text{rms}}$  sine wave from a distance of 3.4 cm. A custom-built class E amplifier was used to drive the power coil from a 5.0-V DC supply. The amplitude of the power signal was modulated to send commands to the IN15 chip at a rate of 16 kb/s. Telemetry data were received with an antenna positioned approximately 6 cm from the IN15 chip. A custom-built 902-928 MHz frequency shift keying (FSK) receiver demodulated the 345.6 kb/s data stream from the IN15 and relayed this information to a PC via a USB interface.

We recorded action potentials with both the IN15 chip and with a conventional Cerebus neural recording system (Cyberkinetics, Inc.) on several different individual intraneural electrodes. The general waveforms and the peak-to-trough amplitudes of the spikes were similar for the two recording systems (Fig. 2). However, the digitized amplifier waveform from the IN15 chip had a DC offset of approximately  $+40 \mu\text{V}$  because of an on-chip device mismatch. The noise level of the IN15 chip recordings ( $23 \mu\text{V}_{\text{rms}}$ ) were also higher than those of the Cerebus ( $6.6 \mu\text{V}_{\text{rms}}$ ), possibly because of interference picked up on the partially unshielded cables connecting the chip to the electrode array (which will not be present in the fully integrated system).

IN15 also performed the first successful on-chip spike detection and spike-detection data transmission. The on-chip spike detector connected to this amplifier uses a 6-bit DAC to set a threshold voltage ranging  $\pm 279 \mu\text{V}$  in  $9 \mu\text{V}$  steps. In one example, we set the spike detection threshold to various levels ranging from  $+45 \mu\text{V}$  to  $+108 \mu\text{V}$  and performed 25-s recording sessions. The left Achilles tendon was repeatedly squeezed and rotated, then released, which likely activated proprioceptive fibers. A stimulus marker switch was depressed approximately coincident with each Achilles tendon stretch, and this marker was recorded in synchrony with the spike detector data. Both the raw neural activity level and the number of on-chip spike detections were highly correlated with the Achilles tendon stimulus (Fig. 3). Spike detection also varied systematically as a function of threshold level (Fig. 4). A discrimination ratio was defined as the ratio of spike rates when the Achilles tendon stimulus was either present or absent. When the spike detection threshold was set too low (e.g.,  $+45 \mu\text{V}$ ), noise triggered the spike detector and discrimination was impossible. When the threshold was set very high (e.g.,  $+108 \mu\text{V}$ ), discrimination was excellent (the spike rate for no stimulus was zero in this case, so the discrimination ratio was infinite), but the number of spikes detected during stimulation was extremely low (0.5 spikes/s).

### C. Cortical Recording

We also successfully tested INI5 in a battery-powered cortical recording application using a variant of the HermesC system developed for long-term neural recording in freely-behaving primates [4]. The INI5 chip was powered from a lithium battery, but telemetry was received wirelessly. Neural signals were obtained from a Cyberkinetics UEA-style array implanted in premotor cortex of a rhesus macaque (monkey D) 3 years prior to this experiment. Cortical action potentials were observed simultaneously using an INI5 with wireless telemetry, as well as a conventional Cerebus recording system. Fig. 5 shows several time-aligned spikes from each system, with post-hoc spike sorting to reveal two distinct units.

Fig. 6 shows an 800-ms trace of neural recording from the Cerebus system (with a 250-Hz high-pass filter applied to the data to approximate the bandwidth of the INI5 amplifiers), the INI5 on-chip 10-bit ADC, and the INI5 on-chip spike detector corresponding to the digitized channel. This spike detector was configured to trigger on electrode voltages falling more than  $99 \mu\text{V}$  below amplifier baseline. Large-amplitude spikes clearly trigger the spike detector, while smaller spikes are ignored. We have shown the estimated threshold as a dashed line in Fig. 6; the exact value of the spike detection threshold cannot be measured directly and will vary slightly from channel to channel because of transistor mismatch.

The noise level of the INI5 chip recordings ( $16 \mu\text{Vrms}$ ) is lower than that in the peripheral nerve recordings, likely due to better shielding. The noise still exceeds the input-referred noise of  $5 \mu\text{Vrms}$  observed in benchtop testing, but some of this excess noise could be background neural activity; the noise levels in the Cerebus recordings are similar ( $15 \mu\text{Vrms}$ ).

### III. SYSTEM INTEGRATION AND ASSEMBLY

In parallel with IC development, we have developed a multi-level hybrid assembly process to integrate a UEA or USEA, INI chip, inductive power receiving coil, and surface-mount device (SMD) capacitors as a monolithic, implantable assembly (Fig. 7a) [1]. This integration concept uses the UEA as a “circuit board”, where the interconnections between components are made through a thin film metal stack which is sputter-deposited on the backside of the UEA (Fig. 7b). The metal traces and pads for SMDs and coil connection were isolated from the silicon substrate by low pressure chemical vapor deposition (LPCVD) of silicon nitride ( $\text{Si}_3\text{N}_4$ ). After silicon nitride deposition, openings for the 100 bond pads were created to make electrical contacts to the UEA electrodes. On these opened bond pads, an under-bump metallization (UBM) using potentially biocompatible materials was sputter-deposited, consisting of a Ti/Pt/Au thin-film stack with layer thicknesses of 50/150/150 nm, respectively. A UBM consisting of Ti/Pt/Au was chosen for compatibility with the Au/Sn solder bumps and because these materials have historically been used for biodevices. The pads and traces for connection to the IC and discrete components were patterned using a lift-off process. A TiW layer with a thickness of 100 nm was deposited after the patterning of the UBM and re-routing traces to serve as a wetting stop layer for the soldering process.

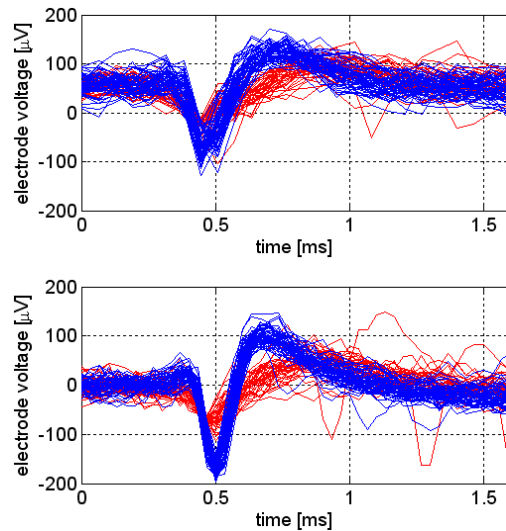


Figure 5. Action potentials recorded from UEA in premotor cortex of rhesus macaque using INI5 chip (top) and conventional Cerebus system (bottom). Two distinct units (sorted manually post-experiment) are visible.

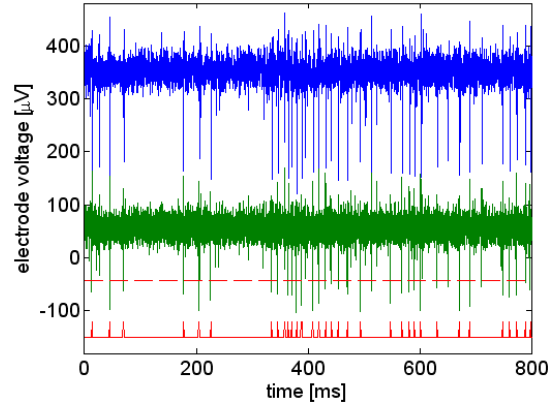


Figure 6. Cortical action potentials recorded simultaneously by conventional Cerebus system (top trace;  $350 \mu\text{V}$  offset added), INI5 10-bit ADC (middle trace), and INI5 on-chip spike detector (bottom trace; binary value). The approximate spike detection threshold is shown as dashed line.

We have built integrated UEA assemblies using various previous versions of INI chips but in this paper, we present the latest assembly process using the INI4 chip. The INI chip was flip-chip bonded to the UEA using Au/Sn reflow soldering at  $340^\circ\text{C}$ . Fig. 8 shows the cross section of Au/Sn bumps at the interconnect between the UEA and IC after reflow soldering. A few discrete SMD capacitors were placed onto the UEA using a pick-and-place tool and connected to the IC by SnCu0.7 reflow soldering at a temperature of up to  $260^\circ\text{C}$  through the re-routing metallization plane. After that, an underfiller was applied between the IC and the UEA to improve mechanical stability and prevent fluid ingress in *in-vivo* conditions. Namics U8433 (NAMICS, Niigata, Japan) was chosen due to its ability to flow into the tight spacing (approximately  $30 \mu\text{m}$ ) between the IC and UEA. The underfill material was dispensed from an applicator at room temperature and flowed into the gap driven by its low viscosity, and by capillary forces. For inductive power and command reception, a flat spiral coil in a diameter of 5.5 mm

was made by winding insulated Au wires in 56  $\mu\text{m}$  diameter (wire thickness with insulation: 66  $\mu\text{m}$ ). The coil has three layers with 30 turns per layer, resulting in an inductance of 29  $\mu\text{H}$ , a series resistance of 16  $\Omega$ , and a quality factor ( $Q$ ) of 31 at 2.765 MHz. The coil thickness was 200  $\mu\text{m}$ . The coil was connected to the INI chip using both a custom-designed ceramic spacer as well as the re-routing plane on the back of the UEA, as shown in Fig. 7. Fig. 9a shows an integrated UEA assembly using the INI4 chip and Au-wire wound coil.

The integrated neural interface device was encapsulated to protect all the components from the aggressive *in-vivo* environment. The encapsulation system used a biocompatible polymer, Parylene-C, which is deposited by chemical vapor deposition (CVD) with a thickness of 3  $\mu\text{m}$ . The Parylene-C acts as a biocompatible layer that protects the device from ions in physiological saline [5]. *In-vitro* encapsulation experiments for fully integrated UEA devices are currently underway.

We have tested the integrated UEA devices after encapsulation in medical grade silicone and Parylene C (Fig. 9b) in *in-vitro* and *in-vivo* conditions. *In-vitro* testing used phosphate buffered saline (PBS) solution to simulate an implanted environment. The effect of immersion in PBS solution on the distance of inductive powering was negligible. For *in-vivo* testing, one integrated UEA device was acutely implanted in cat cerebral cortex and another in sciatic nerve. The UEA device was functional when the power transmit coil was up to 7 mm from the skin surface, sending an RF carrier signal at 904 MHz, indicating that power transmission was successful. The depth of the UEA assembly below the skin was measured to be 10 mm, resulting in a coil-to-coil transmission distance of 18 mm.

#### IV. CONCLUSIONS

We have demonstrated a single-chip neural recording device that performs on-chip amplification, digitization, spike detection, and wireless telemetry. Spike detection thresholds may be adjusted independently for each of 100 channels, giving users the flexibility to detect spikes and reject background noise and neural hash. Initial *in-vivo* experiments confirm functionality of the IC in both peripheral and central nervous system applications.

The chip can be bonded to the back on a 100-electrode UEA or USEA along with several surface-mount passive components (e.g., capacitors too large for integration) and a small coil for receiving power, clock, and command signals remotely through an inductive link. A previous version of the INI chip has been fully integrated, implanted in both cortex and nerve, and powered wirelessly from a coil-to-coil distance of 18 mm.

#### REFERENCES

[1] M. Töpper et al., "Biocompatible Hybrid Flip Chip Microsystem integration for next generation wireless neural interfaces," In: *Proc. 2006 IEEE Electronic Components and Technology Conference*, San Diego, CA, pp. 705-708, 2006.

[2] R.R. Harrison et al., "A low-power integrated circuit for a wireless 100-electrode neural recording system," *IEEE J. Solid-State Circuits*, vol. 42, pp. 123-133, January 2007.

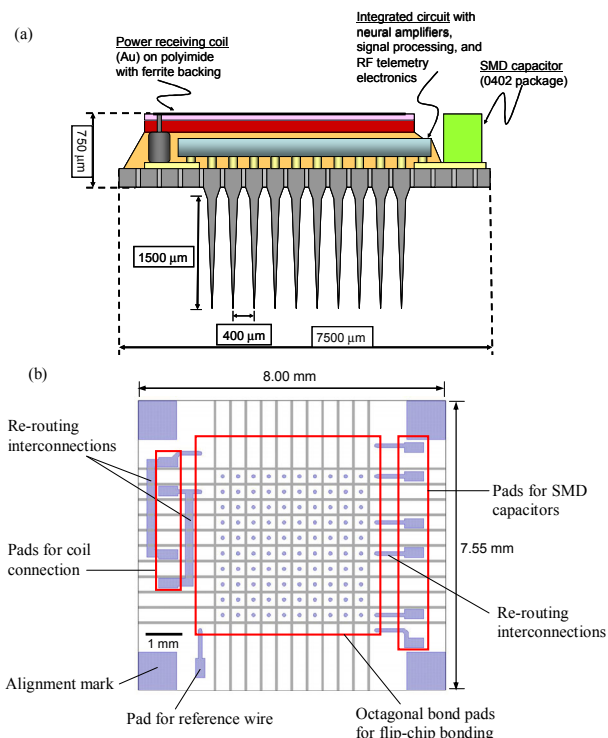


Figure 7. (a) Schematic of the integration and packaging concept of an integrated wireless neural interface. (b) Layout of the UBM and re-routing metallization serving as a circuit board to interconnect the UEA, IC, coil and SMD components. The back plate of the UEA measures  $8.00 \times 7.55 \text{ mm}^2$ .

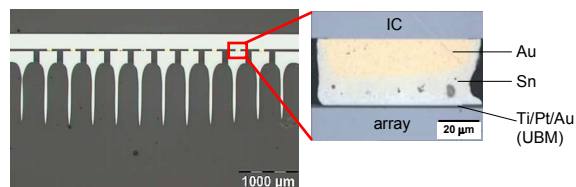


Figure 8. Optical micrographic images of the cross section of Au/Sn bumps at the interconnect with the array after reflow soldering.

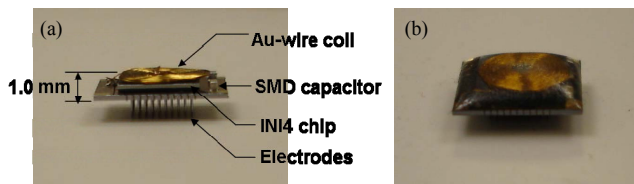


Figure 9. Photographs of Integrated Neural Interface used for *in-vivo* testing (a) before encapsulation and (b) after encapsulation in silicone and 3- $\mu\text{m}$  Parylene. Dimensions are  $7.6 \times 8.0 \text{ mm}$ , with an overall height of 2.5 mm including the electrodes. The silicone layer adds 0.7 mm to the thickness.

[3] R.R. Harrison et al., "Wireless neural signal acquisition with single low-power integrated circuit," In: *Proc. 2008 IEEE Intl. Sym. Cir. & Sys. (ISCAS 2008)*, Seattle, WA, pp. 1748-1751, 2008.

[4] C.A. Chestek et al., "HermesC: RF wireless low-power neural recording for freely behaving primates," In: *Proc. 2008 IEEE Intl. Sym. Cir. & Sys. (ISCAS 2008)*, Seattle, WA, pp. 1752-1755, 2008.

[5] J.-M. Hsu, L. Rieth, R.A. Normann, P. Tathireddy, and F. Solzbacher, "Hermetic encapsulation of an integrated neural interface device with Parylene-C," to appear in *IEEE Trans. Biomed. Eng.*